

**The following resources related to this article are available online at
www.sciencemag.org (this information is current as of July 30, 2009):**

Updated information and services, including high-resolution figures, can be found in the online version of this article at:

<http://www.sciencemag.org/cgi/content/full/325/5939/477>

Supporting Online Material can be found at:

<http://www.sciencemag.org/cgi/content/full/1175088/DC1>

This article **cites 32 articles**, 19 of which can be accessed for free:

<http://www.sciencemag.org/cgi/content/full/325/5939/477#otherarticles>

This article has been **cited by** 1 articles hosted by HighWire Press; see:

<http://www.sciencemag.org/cgi/content/full/325/5939/477#otherarticles>

This article appears in the following **subject collections**:

Cell Biology

http://www.sciencemag.org/cgi/collection/cell_biol

Information about obtaining **reprints** of this article or about obtaining **permission to reproduce this article** in whole or in part can be found at:

<http://www.sciencemag.org/about/permissions.dtl>

of the National MPS Society USA are gratefully acknowledged. The authors have no conflicts of interest. Expression microarray data are available at the Gene Expression Omnibus repository under accession number GSE16267. A patent application on the discovery of a gene network regulating lysosomal biogenesis and function has been filed to the European Patent Office

(patent application EP 091527788). A.B. and M.S. are inventors on this patent.

Supporting Online Material

www.sciencemag.org/cgi/content/full/1174447/DC1
Materials and Methods
Figs. S1 to S12

Tables S1 to S5
References

2 April 2009; accepted 10 June 2009
Published online 25 June 2009;
10.1126/science.1174447
Include this information when citing this paper.

An ER-Mitochondria Tethering Complex Revealed by a Synthetic Biology Screen

Benoît Kornmann,^{1*} Erin Currie,^{1†} Sean R. Collins,^{2,3‡} Maya Schuldiner,⁴ Jodi Nunnari,⁵ Jonathan S. Weissman,^{2,3} Peter Walter^{1,3}

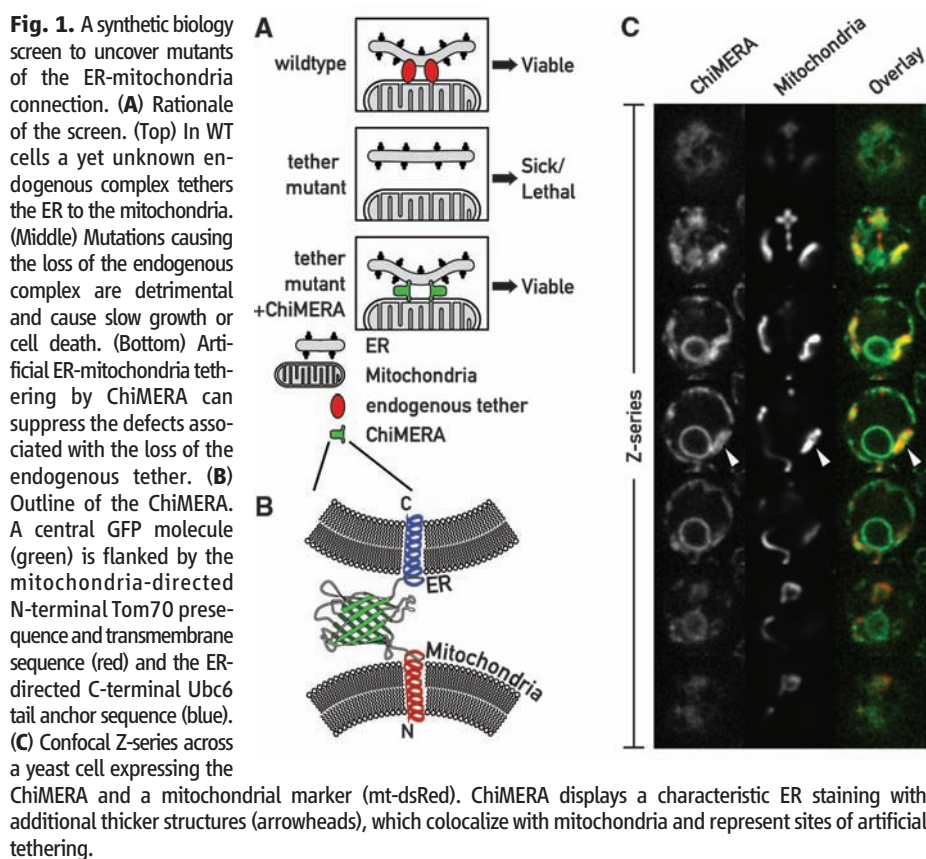
Communication between organelles is an important feature of all eukaryotic cells. To uncover components involved in mitochondria/endoplasmic reticulum (ER) junctions, we screened for mutants that could be complemented by a synthetic protein designed to artificially tether the two organelles. We identified the Mmm1/Mdm10/Mdm12/Mdm34 complex as a molecular tether between ER and mitochondria. The tethering complex was composed of proteins resident of both ER and mitochondria. With the use of genome-wide mapping of genetic interactions, we showed that the components of the tethering complex were functionally connected to phospholipid biosynthesis and calcium-signaling genes. In mutant cells, phospholipid biosynthesis was impaired. The tethering complex localized to discrete foci, suggesting that discrete sites of close apposition between ER and mitochondria facilitate interorganelle calcium and phospholipid exchange.

Eukaryotic cells evolved segregation of functions into separate organelles. Compartmentalization increases the efficiency of biochemical reactions by creating tailored chemical microenvironments, but also creates a need for communication and routes of metabolite exchange. Membrane lipids, for example, are primarily synthesized in the endoplasmic reticulum (ER) and distributed to other organelles. Many organelles exchange phospholipids with the ER via vesicular transport. In contrast, mitochondria are not connected to vesicular trafficking pathways, and many lipids of the inner and outer mitochondrial membranes (IMM and OMM) cannot be synthesized within mitochondria but are imported by unclear mechanisms. Phospholipids may transfer from the ER to the OMM at spatially restricted sites, which are frequently observed by electron microscopy and have been enriched by cell fractionation (1–3).

Other work has implicated ER-mitochondrial contact sites in Ca^{++} transport between the ER and mitochondria (4–6), suggesting a mecha-

nism that may exploit the formation of an encapsulated space at the contact sites, akin to that formed at neuronal or immunological synapses. Such a connection between the ER and the mitochondria might buffer and control cytosolic and mitochondrial Ca^{++} concentrations (7). Several proteins have been implicated to participate in ER-mitochondria contacts, including the ER resident Ca^{++} channel IP3 receptor, the mitochondrial voltage-dependent anion channel, the chaperones grp75 and sigma-1R, the sorting protein PACS-2, and the mitofusin Mfn2 (8–11).

To explore a role for ER-mitochondrial junctions, we sought mutants in the yeast *Saccharomyces cerevisiae*, in which tethering between the two organelles was impaired. We reasoned that, if such contacts are important, defects in proteins that establish these interactions would be detrimental, yet perhaps could be suppressed by artificially tethering ER and mitochondria (Fig. 1A). We designed a synthetic ER-mitochondria tether (“ChiMERA” for construct helping in mitochondria-ER association) (Fig. 1B) consisting of an N-terminal mitochondrial signal sequence and transmembrane domain derived



¹Department of Biochemistry and Biophysics, University of California at San Francisco, San Francisco, CA 94158, USA.

²Department of Cellular and Molecular Pharmacology, University of California at San Francisco, San Francisco, CA 94158, USA. ³Howard Hughes Medical Institute, University of California at San Francisco, San Francisco, CA 94158, USA.

⁴Molecular Genetics, Weizmann Institute of Science, Rehovot, Israel. ⁵Molecular and Cellular Biology, University of California at Davis, Davis, CA 95616, USA.

*To whom correspondence should be addressed. E-mail: benoit.kornmann@ucsf.edu

†Present address: Gladstone Institute of Cardiovascular Disease, San Francisco, CA 94158, USA.

‡Present address: Chemical and Systems Biology, Bio-X Program, Stanford University, Stanford, CA 94305, USA.

from Tom70, a central module composed of green fluorescent protein (GFP), and a C-terminal ER tail-anchor derived from Ubc6. The design was based on a similar chimeric protein that strengthened mitochondria-ER interactions (12). The GFP moiety allowed us to visualize its tethering activity directly (Fig. 1C and fig. S1A). ChiMERA localized mainly to ER membranes and stained both peripheral and perinuclear ER. In addition, ChiMERA localized to patches of contact with mitochondria (Fig. 1C). Mitochondria in untransformed wild-type (WT) cells showed the characteristic morphology of a uniformly tubular network (Fig. 2B and fig. S1B) and adopted a pronounced patchy structure at the artificial contact sites in cells expressing ChiMERA (Fig. 1C and fig. S1A; see also Fig. 2B). Thus, ChiMERA tethers mitochondria and ER as intended. The dominant ER staining probably reflects a partial dominance of the ER targeting sequence over the mitochondrial one. We also generated a second version of the artificial tether in which the yeast Tom70 presequence and transmembrane domain was replaced by the mouse AKAP1 presequence (12). This construct also localized predominantly to the ER but accumulated in only one to three discrete foci per cell (fig. S2). These foci colocalized with both ER (fig. S2A) and mitochondria (fig. S2B). This construct, however, did not create distortions in mitochondrial shape. It is likely that this synthetic protein does not exert a substantial tethering force and instead labels preexisting ER-mitochondrial interfaces. We refer to this construct as ChiMERA-ra (for ChiMERA with reduced affinity).

We next used a construct expressing ChiMERA from a centromeric expression plasmid in a classical sectoring screen (13). We screened ~100,000 ethylmethanesulfonate-treated colonies and retrieved two mutants that could not grow in the absence of the plasmid. Genetic complementation (14) indicated that the mutations are two different alleles of *MDM12*. Accordingly, a strain bearing a complete deletion of *MDM12* grew on respiration plates when it expressed the ChiMERA, but the strain failed to grow without it (Fig. 2A). Mdm12 is a peripheral OMM protein (15) (fig. S3). Mdm12 can be isolated from cell extracts as a complex with Mmm1 and Mdm10 and localizes in a few punctate structures along the mitochondrial network, together with a fourth protein, Mdm34 (16, 17) (Fig. 3A). All four proteins are required for respiratory growth and for the maintenance of the proper tubular morphology of mitochondria. We deleted *MMM1*, *MDM10*, and *MDM34* and assessed the extent to which ChiMERA could rescue their phenotypes. ChiMERA expression partially suppressed growth defects, albeit to highly different extents (Fig. 2A). *mdm12Δ*, *mmm1Δ*, *mdm10Δ*, and *mdm34Δ* strains displayed enlarged and spherical mitochondria as compared with the tubular WT mitochondria (18). ChiMERA expression also restored the mitochondrial morphology of *mdm12Δ* and *mdm34Δ* strains (Fig. 2B and fig. S4), although it

failed to do so in *mmm1Δ* and *mdm10Δ* strains, consistent with the lesser rescue of growth on respiration medium (Fig. 2A). An Mdm34-mCherry fusion protein colocalized with both the punctate structures labeled by ChiMERA-ra and the broad ER-mitochondria interfaces created by ChiMERA (fig. S5).

Thus, one core molecular function of the Mmm1/Mdm10/Mdm12/Mdm34 complex is to connect ER and mitochondria, which can be bypassed by expressing a synthetic tether. Henceforth, we refer to the complex as ERMES (ER-mitochondria encounter structure).

ERMES localizes into a few discrete foci (16, 17), and mutations in any single component cause the puncta to disappear (16, 17). We reasoned that ERMES components may be respectively localized to the ER and mitochondria, and they might serve to zipper the organelles together. ERMES disruption would then cause some of the components to partition with ER, whereas some others would partition with mitochondria.

To address this possibility, we replaced the gene encoding each ERMES component with that of a functional GFP fusion protein and imaged both WT and mutant cells (Fig. 3A). In WT cells, ERMES components displayed the expected punctate pattern, with the exception of Mdm10, which displayed a more widespread localization throughout the mitochondrial network. This is consistent with the observation that Mdm10 is not only a component of ERMES but is also a component of the sorting and assembly machinery (SAM) complex in the OMM (19). As expected from its assignment as an OMM protein, Mdm34-GFP relocalized uniformly to mitochondria in the absence of Mdm10, Mdm12, and Mmm1 (Fig. 3A; note the swollen morphology of

mitochondria in the mutants). Likewise, Mdm10-GFP remained colocalized with mitochondria in all strains tested. In contrast, and contrary to expectation, Mmm1-GFP relocalized to the ER, showing a characteristic peripheral and perinuclear staining in the absence of Mdm10, Mdm12, or Mdm34. Mdm12-GFP, a membrane peripheral protein (fig. S3), relocalized to the ER in the absence of Mdm10 or Mdm34, and the mitochondria in the absence of Mmm1, suggesting that its localization depends on the availability of interaction partners at either organelle.

Mmm1 harbors a classical helical transmembrane domain, previously proposed to be inserted into either the outer or inner mitochondrial membrane (20), yet our localization data suggested that Mmm1 is instead inserted into the ER. Many integral ER membrane proteins are N-glycosylated within their luminal domains, and four potential N-glycosylation sites lie in the N terminus of Mmm1 preceding the transmembrane domain. To address whether these sites were glycosylated, we replaced the *MMM1* gene with fully functional hemagglutinin (HA)-tagged *MMM1* and assessed the electrophoretic mobility of HA-Mmm1 from cell extracts with or without treatment with the glycosidase EndoH_f, which removes N-linked glycans. Treatment with EndoH_f caused HA-Mmm1 to migrate faster (Fig. 3B and fig. S6A), indicating that Mmm1 is N-glycosylated and therefore is an integral ER membrane protein that was misannotated as a mitochondrial protein. The misannotation was partly due to the interpretation of a tobacco etch virus (TEV) protease cleavage accessibility assay (20). We used the same assay with an ER-targeted TEV protease and confirmed Mmm1 ER-membrane insertion (fig. S6B).

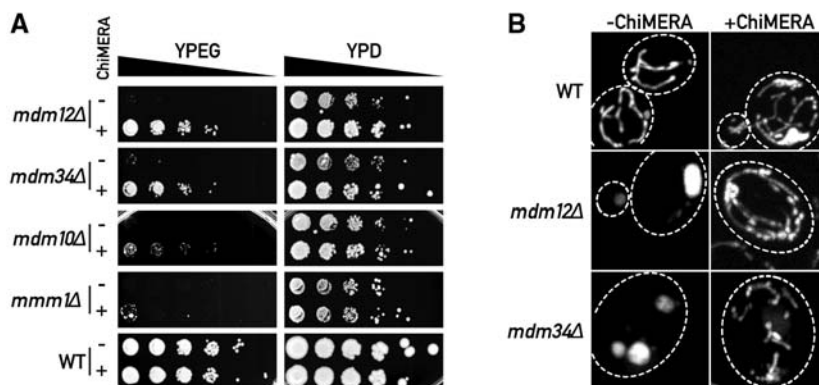


Fig. 2. ChiMERA expression suppresses phenotypes associated with deletions of ERMES complex components. **(A)** 10-fold serial dilutions of a saturated culture were spotted on YP + ethanol/glycerol medium (YPEG) that supports growth by respiration or YP + dextrose (YPD) that allows fermentation. ChiMERA expression rescues growth of *mdm12Δ*, *mdm34Δ*, *mdm10Δ*, and *mmm1Δ* strains to different extents on respiration medium. **(B)** The mitochondrial shape defect of *mdm12Δ* and *mdm34Δ* strains is partially suppressed by expression of the ChiMERA. Cells bearing a mitochondria-targeted dsRed were imaged with the use of confocal fluorescence microscopy. Z projections across the whole volume of the cells are shown. A broken white line outlines the perimeter of the cell. ChiMERA expression has no effect in WT cells, other than formation of artificial tethering structures. *mdm12Δ* and *mdm34Δ* strains display rounded and enlarged mitochondria. The mitochondrial tubular shape is substantially restored upon ChiMERA expression. A quantitation of this effect is shown in fig. S4.

Taken together, our results indicate that ERMES functions as a molecular zipper bridging between ER and mitochondria. ERMES consists of the ER-resident membrane protein Mmm1 and the OMM-resident β -barrel protein Mdm10 (21). The well-characterized interaction of these two proteins (16, 19) requires Mdm12 and Mdm34. Defects in these latter proteins can be compensated by expressing ChiMERA, a synthetic protein that bridges ER and mitochondrial membranes, strongly suggesting that one primary physiological role of ERMES is that of a mechanical tether. Mutation of a single ERMES component causes complex disassembly but results in different growth phenotypes. Deletions of *MDM12* and *MDM34* are easily compensated for by ChiMERA expression, whereas deletions of *MMM1* and *MDM10* are less efficiently compensated. The variability in phenotypes indicates that Mmm1 and Mdm10 still provide useful activity in the absence of a functional complex, provided that an artificial tether is

present. Mdm10 is a component of both ERMES and of the SAM complex (19) that imports β -barrel proteins in the OMM, and therefore, this latter activity would not be expected to be compensated for by ChiMERA expression.

From these results, it appeared plausible that impairing ER-mitochondrial tethering provided the molecular basis for the phenotypes associated with ERMES defects, thus offering a unique opportunity to investigate the physiology of ER-mitochondria communication. To evaluate systematically the phenotypic consequences of loss of ERMES, we analyzed a recently generated epistasis mini-array profile (E-MAP) (see supplement) (22). The E-MAP methodology identifies functionally related genes by comparing their profiles of genetic interaction. In the map, a set of 1493 null or hypomorphic alleles, including *mmm1 Δ* , *mdm10 Δ* , *mdm12 Δ* , and *mdm34 Δ* strains, was crossed to a set of 484 query null or hypomorphic strains selected primarily for their association with

mitochondrial and ER biology. The phenotype of the ~700,000 double mutants was assessed by colony size and used to calculate quantitative genetic interactions. This analysis confirmed previously characterized genetic interactions. For instance, prohibitins (*PHB1* and *PHB2*), which have been shown to be synthetic lethal to ERMES component deletions (23), display some of the strongest synthetic phenotypes (Fig. 4A).

We used the interaction patterns of the 1493 genes in this analysis to calculate pairwise correlation coefficients. In this analysis, genes encoding ERMES components consistently showed strong correlation with each other (Fig. 4B), confirming that these genes are functionally related and that this analysis has the power to uncover this relation. Two genes, *GEM1* and *PSD1*, showed strong correlation to every ERMES gene. Gem1 is a calcium-binding rho-like GTPase inserted in the OMM and involved in calcium-dependent mitochondrial movement and inheritance (24, 25). Psd1 is a phosphatidylserine (PS) decarboxylase involved in the de novo biosynthesis of aminoglycerophospholipids. ER-mitochondria connections have been previously shown to be important for interorganelle calcium and phospholipid exchange, further supporting a role for ERMES in mediating ER-mitochondrial junctions.

The phenotypic similarity between ERMES and *PSD1* was particularly notable because Psd1 is the only aminoglycerophospholipid biosynthetic enzyme in mitochondria (1) (fig. S7), implying that its substrate has to be transported from the ER and its product back to the ER. To assess a role of ER-mitochondrial junctions in lipid biosynthesis, we first analyzed mitochondrial phospholipid content in ERMES-disrupted (*mdm12 Δ*) cells at steady-state conditions. All phospholipid classes were represented in ratios comparable to those of WT cells, with the notable exception of cardiolipin (CL), which was much reduced in its relative abundance (Fig. 4C). CL is a mitochondria-specific phospholipid essential for respiration. Deletion of any ERMES component, as well as of *PSD1*, is synthetically lethal with a deletion of *CRD1* (Fig. 4A) (26), which encodes the CL synthase (27). Moreover, *psd1 Δ* cells also display reduced CL levels (28). Thus, similar to *psd1 Δ* cells, ERMES mutant strains suffer from mitochondrial phospholipid abnormalities and cannot tolerate the absence of a functional CL biosynthesis pathway, even when grown in fermentable medium. In addition, an extensive cross talk has been observed between aminoglycerophospholipid and CL synthesis, along with a reduction in CL levels in *mmm1 Δ* , *mdm10 Δ* , and *mdm34 Δ* strains (23).

The maintenance of a balance between most phospholipid species besides CL in *mdm12 Δ* mutant cells suggests that ER-mitochondria connections might affect the rate of phospholipid biosynthesis but have little effect on steady-state levels because of compensatory mechanisms (28). To assess this possibility, we monitored the

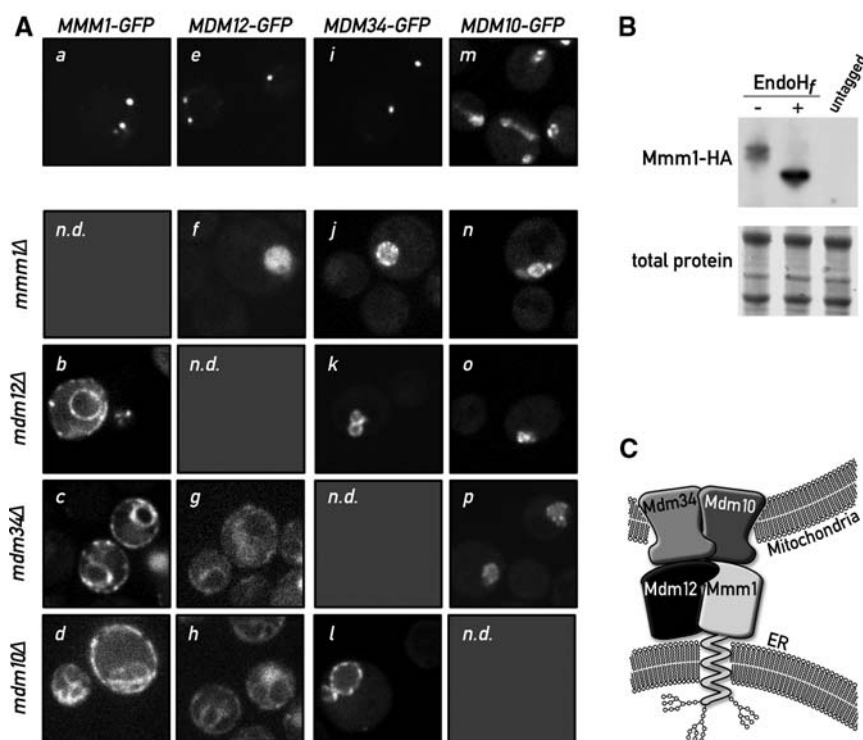
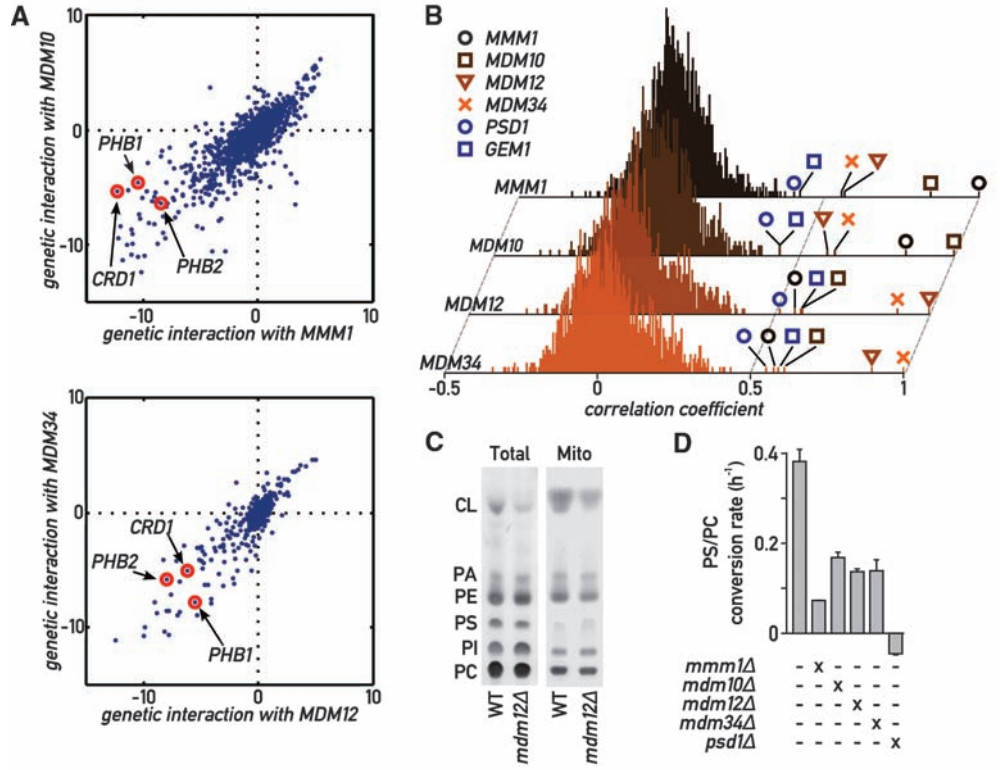


Fig. 3. Mmm1 is an integral ER protein. **(A)** Disruption of a single ERMES component causes disassembly of the complex. Mmm1-GFP is localized in punctate structures in WT cells (a). Upon deletion of *MDM12* (b), *MDM34* (c), or *MDM10* (d), Mmm1-GFP relocates to the ER. Mdm12-GFP displays a punctate pattern in WT cells (e). In the absence of Mmm1 (f), Mdm12-GFP displays a uniform mitochondrial localization (note the rounded swollen mitochondrial shape in *mmm1 Δ* strains), but in the absence of *MDM34* (g) or *MDM10* (h), Mdm12-GFP relocates to the ER. Mdm34-GFP is also in punctate structures in WT cells (i). Upon mutation of any other complex member, Mdm34 relocates more uniformly to the mitochondrial membrane (j, k, l). Mdm10-GFP localizes to the whole surface of the mitochondria (m) and localizes to the rounded mitochondria after deletion of any other ERMES component (n, o, p). n.d., not determined. **(B)** Mmm1 is N-glycosylated. Whole-cell extract from a strain bearing a functional HA-tagged *MMM1* gene was subjected to SDS-polyacrylamide gel electrophoresis with or without pretreatment with the glycosidase *EndoH_f*. Detection was performed by Western blotting with an anti-HA antibody. The shift in electrophoretic mobility upon glycosidase treatment is indicative that Mmm1 is N-linked glycosylated. **(C)** Model of ERMES-mediated ER-mitochondria tethering. Mmm1 is an integral ER protein glycosylated on its N-terminal side. Mmm1 interacts with Mdm10, an OMM β -barrel protein. Mdm34 and Mdm12 promote this association, most probably via direct association.

Fig. 4. Global analysis of ERMES genetic interactions. **(A)** Genetic interactions of *MMM1* and *MDM10* (top) and of *MDM12* and *MDM34* (bottom). Positive values indicate epistatic or suppressive interactions (i.e., double mutant grows better than expected from the combination of the phenotypes of each single mutant); negative values indicate a synthetic sick/lethal genetic interaction (i.e., double mutant grows worse than expected). **(B)** Histograms of correlation coefficients generated by comparing the profiles of genetic interaction for each ERMES component to all other 1493 profiles in the E-MAP analysis. ERMES components display strongest correlation to each other and to *GEM1* and *PSD1*. **(C)** Thin-layer chromatography (TLC) analysis of steady-state total and mitochondrial phospholipids in WT and *mdm12Δ* strains. PA, phosphatidic acid; PI, phosphatidylinositol. **(D)** The aminoglycerophospholipid biosynthesis pathway is slowed down in ERMES mutants. Cultures of the indicated genotypes were labeled with ¹⁴C-serine, then chased with an excess cold serine. The variation of the PC/PS ratio was then measured over time by quantitative TLC, and its slope was estimated with linear regression. Error bars represent the SE of the linear regression.



conversion of PS to phosphatidylcholine (PC) in a ¹⁴C-serine pulse-chase. This experiment was conducted in a *psd2Δ* background to exclude the contribution of the vacuolar PS decarboxylase *Psd2* (29). An otherwise WT strain displayed a high rate of PS-to-PC conversion (Fig. 4E), whereas a *psd1Δ psd2Δ* strain failed to convert PS to PC. Mutants of ERMES showed a two- to fivefold reduction in PS-to-PC conversion rate (Fig. 4D), consistent with the notion that disruption of ERMES impairs phospholipid exchange between ER and mitochondria. This defect was partially reversed by ChiMERA expression in *mdm12Δ psd2Δ* and *mdm34Δ psd2Δ* strains (fig. S8). Contrary to *psd1Δ psd2Δ* strains, however, none of the *psd2Δ* ERMES mutants were auxotrophic for ethanolamine, showing that, consistent with the pulse-chase labeling data, *Psd1* still displayed activity even in the absence of tethering.

Thus, ERMES-mediated ER-mitochondria connections are necessary for efficient inter-organelle phospholipid exchange. A reduced rate of lipid exchange in turn slows down aminoglycerophospholipid turnover, which results in impaired CL synthesis (28). It is likely that part of the pronounced defects in ERMES mutant cells results from problems in mitochondrial membrane maintenance (23).

Our strategy of discovering unknown genes by encoding their function into artificial constructs may be applicable to other situations in which a synthetic protein can substitute for an endogenous gene(s).

Mmm1 and *Mdm12* belong to the SMP-domain protein family that has multiple members across all eukaryotes (30), making it likely that complexes containing one or more of these SMP-domain-containing proteins perform similar functions in metazoan cells.

The organization of the ERMES complex into 2 to 10 foci per cell suggests that the number and extent of interorganelle exchange surfaces have been vastly overestimated (2), or that eukaryotes may have evolved multiple specialized and spatially restricted structures that perhaps are dedicated to particular tasks. Each ERMES punctum represents a large macromolecular assembly that is expected to contain, for example, ~250 molecules of *Mmm1* (31). The mechanical tethering provided by ERMES might organize specialized membrane domains that serve as platforms to recruit other molecules, which, in turn, carry out the physiological roles of the junctions, such as lipid transport or calcium exchange. ERMES foci localize adjacent to actively replicating mitochondrial nucleoids, as part of a poorly characterized assembly spanning both OMM and IMM (32). Such structures would span a third membrane and thus could strategically connect the ER lumen and the mitochondrial genome. The purpose of such a link is unclear, but we can speculate that it might help coordinate mitochondrial growth by coupling mitochondrial genome replication and membrane upkeep. In this light, the presence of *Mdm10* in both SAM and ERMES complexes provides the intriguing possibility that such a link includes regulation of mitochondrial protein import.

References and Notes

1. D. R. Voelker, *J. Lipid Res.* **44**, 441 (2003).
2. G. Achleitner et al., *Eur. J. Biochem.* **264**, 545 (1999).
3. J. E. Vance, *J. Biol. Chem.* **266**, 89 (1991).
4. R. Rizzuto, A. W. Simpson, M. Brini, T. Pozzan, *Nature* **358**, 325 (1992).
5. R. Rizzuto, M. Brini, M. Murgia, T. Pozzan, *Science* **262**, 744 (1993).
6. R. Rizzuto et al., *Science* **280**, 1763 (1998).
7. P. Pinton et al., *Oncogene* **27**, 6407 (2008).
8. T. Simmen et al., *EMBO J.* **24**, 717 (2005).
9. G. Szabadkai et al., *J. Cell Biol.* **175**, 901 (2006).
10. T. Hayashi, T. Su, *Cell* **131**, 596 (2007).
11. O. M. de Brito, L. Scorrano, *Nature* **456**, 605 (2008).
12. G. Csordás et al., *J. Cell Biol.* **174**, 915 (2006).
13. P. Hieter, C. Mann, M. Snyder, R. W. Davis, *Cell* **40**, 381 (1985).
14. M. D. Rose, J. R. Broach, *Methods Enzymol.* **194**, 195 (1991).
15. K. H. Berger, L. F. Sogo, M. P. Yaffe, *J. Cell Biol.* **136**, 545 (1997).
16. I. R. Boldogh et al., *Mol. Biol. Cell* **14**, 4618 (2003).
17. M. J. Youngman et al., *J. Cell Biol.* **164**, 677 (2004).
18. S. J. McConnell, L. C. Stewart, A. Talin, M. P. Yaffe, *J. Cell Biol.* **111**, 967 (1990).
19. C. Meisinger et al., *EMBO J.* **26**, 2229 (2007).
20. N. Kondo-Okamoto, J. M. Shaw, K. Okamoto, *J. Biol. Chem.* **278**, 48997 (2003).
21. S. Kutik et al., *Cell* **132**, 1011 (2008).
22. M. Schuldiner et al., *Cell* **123**, 507 (2005).
23. C. Osman et al., *J. Cell Biol.* **184**, 583 (2009).
24. X. Wang, T. L. Schwarz, *Cell* **136**, 163 (2009).
25. R. L. Frederick et al., *J. Cell Biol.* **167**, 87 (2004).
26. V. M. Gohil, M. N. Thompson, M. L. Greenberg, *J. Biol. Chem.* **280**, 35410 (2005).
27. S. C. Chang et al., *J. Biol. Chem.* **273**, 14933 (1998).
28. R. Birner, M. Bürgermeister, R. Schneiter, G. Daum, *Mol. Biol. Cell* **12**, 997 (2001).
29. P. J. Trotter, D. R. Voelker, *J. Biol. Chem.* **270**, 6062 (1995).
30. I. Lee, W. Hong, *FASEB J.* **20**, 202 (2006).
31. S. Ghaemmaghami et al., *Nature* **425**, 737 (2003).

32. S. Meeusen, J. Nunnari, *J. Cell Biol.* **163**, 503 (2003).
 33. We thank all members of the Walter lab for their support; N. Krogan, S. Wang, and N. Bajwa for their work creating the genetic interaction maps; and J. Shaw and K. Okamoto for their kind gift of plasmids and discussions. This work was supported by NIH. B.K. is a fellow of the Swiss National Science Foundation; M.S. is supported by a Human Frontiers Science Program Career Development Award; and

P.W. and J.S.W. are investigators at the Howard Hughes Medical Institute.

References
 Database S1

Supporting Online Material

www.sciencemag.org/cgi/content/full/1175088/DC1
 Materials and Methods
 Figs. S1 to S8
 Tables S1 and S2

17 April 2009; accepted 8 June 2009

Published online 25 June 2009;

10.1126/science.1175088

Include this information when citing this paper.

Pathogenesis and Transmission of Swine-Origin 2009 A(H1N1) Influenza Virus in Ferrets

Vincent J. Munster,^{1*} Emmie de Wit,^{1*} Judith M. A. van den Brand,¹
 Sander Herfst,¹ Eefje J. A. Schrauwen,¹ Theo M. Bestebroer,¹ David van de Vijver,¹
 Charles A. Boucher,¹ Marion Koopmans,^{1,2} Guus F. Rimmelzwaan,¹ Thijs Kuiken,¹
 Albert D. M. E. Osterhaus,¹ Ron A. M. Fouchier^{1†}

The swine-origin A(H1N1) influenza virus that has emerged in humans in early 2009 has raised concerns about pandemic developments. In a ferret pathogenesis and transmission model, the 2009 A(H1N1) influenza virus was found to be more pathogenic than a seasonal A(H1N1) virus, with more extensive virus replication occurring in the respiratory tract. Replication of seasonal A(H1N1) virus was confined to the nasal cavity of ferrets, but the 2009 A(H1N1) influenza virus also replicated in the trachea, bronchi, and bronchioles. Virus shedding was more abundant from the upper respiratory tract for 2009 A(H1N1) influenza virus as compared with seasonal virus, and transmission via aerosol or respiratory droplets was equally efficient. These data suggest that the 2009 A(H1N1) influenza virus has the ability to persist in the human population, potentially with more severe clinical consequences.

In April 2009, swine-origin 2009 A(H1N1) influenza virus [2009 A(H1N1) influenza virus] was recognized as the causative agent of influenza-like illnesses in humans in North America (1–3). Since then, 76 countries have officially reported 35,928 cases of 2009 A(H1N1) influenza virus infection, including 163 deaths (4). The 2009 A(H1N1) influenza virus contains a previously unseen combination of gene segments from the North American and Eurasian swine influenza virus lineages (1, 5). The virus has apparently circulated in the swine population without detection and recently crossed the species barrier into humans. The most recent common ancestor of the human 2009 A(H1N1) influenza viruses was estimated to have emerged between November 2008 and March 2009. One of the unusual characteristics of the 2009 A(H1N1) influenza virus as compared with other recent zoonotic influenza viruses is sustained human-to-human transmission, with basic reproduction ratio (R_0) estimates in the range of 1.2 to 1.6, which is higher than that reported for seasonal human influenza A viruses (1). In response to the available informa-

tion on sustained human-to-human transmission in multiple parts of the world, the World Health Organization (WHO) raised the level of influenza pandemic alert to phase 6 on 11 June 2009 (6).

Currently available data indicate that the majority of laboratory-confirmed infections with the

2009 A(H1N1) influenza virus result in a self-limiting, uncomplicated influenza (2, 3, 7). Typical clinical symptoms include fever, rhinorrhea, cough, and sore throat, which are indistinguishable from the symptoms observed for seasonal A(H1N1) and A/H3N2 influenza virus infections. However, in addition to uncomplicated influenza, a variety of clinical symptoms unusual for seasonal influenza have been described, including vomiting and diarrhea in a relatively large proportion of cases. Moreover, some patients have required hospitalization because of severe pneumonia and respiratory failure, with a fatal outcome occurring in 0.5% of laboratory-confirmed cases. In contrast to seasonal influenza, a substantial proportion of the cases of severe illness and death have occurred among young and previously healthy adults. Severe illness and deaths have also been noted relatively frequently in adults with underlying disease and in pregnant women (2, 3, 7).

The distinct antigenic properties of the 2009 A(H1N1) influenza virus as compared with seasonal A(H1N1) virus suggests that population humoral immunity against pandemic 2009 A(H1N1) influenza virus is limited (5), although the age distribution of reported cases suggests some degree of protection in older age groups (1–3).

We used a ferret (*Mustela putorius furo*) model to study clinical signs, virus shedding, tissue distribution, pathology, and aerosol transmission

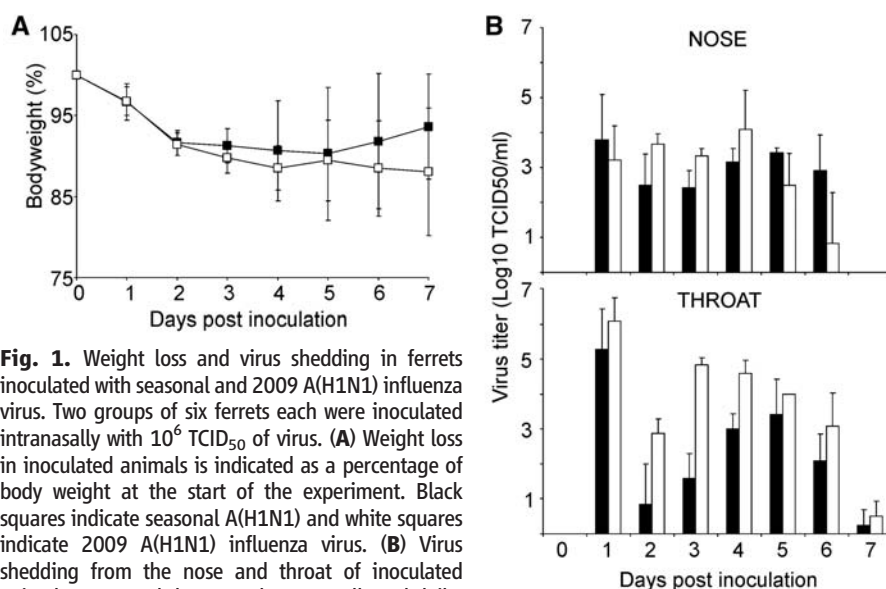


Fig. 1. Weight loss and virus shedding in ferrets inoculated with seasonal and 2009 A(H1N1) influenza virus. Two groups of six ferrets each were inoculated intranasally with 10^6 TCID₅₀ of virus. **(A)** Weight loss in inoculated animals is indicated as a percentage of body weight at the start of the experiment. Black squares indicate seasonal A(H1N1) and white squares indicate 2009 A(H1N1) influenza virus. **(B)** Virus shedding from the nose and throat of inoculated animals. Nose and throat swabs were collected daily, and virus titers in the swabs were determined by means of end-point titration in MDCK cells. Geometric mean titers are displayed; error bars indicate SD. Black bars indicate seasonal A(H1N1) and white bars indicate 2009 A(H1N1) influenza virus.

¹National Influenza Center and Department of Virology, Erasmus Medical Center, 3015GE Rotterdam, Netherlands.
²National Institute for Public Health and the Environment, 3720BA Bilthoven, Netherlands.

*These authors contributed equally to this work.

†To whom correspondence should be addressed. E-mail: r.fouchier@erasmusmc.nl